Article

SOURCE DATA | TRANSPARENT PROCESS

EMBO reports

MYC promotes cancer progression by modulating m^{6}A modifications to suppress target gene translation

Gongwei Wu[1,2,*,†,‡], Caixia Suo[1,3,†], Ying Yang[4], Shengqi Shen[2], Linchong Sun[1,3], Shi-Ting Li[2], Yingli Zhou[2], Dongdong Yang[2], Yan Wang[2], Yongping Cai[5], Nana Wang[5], Huafeng Zhang[2], Yun-Gui Yang[4,6,7,8,**], Jie Cao[1,3,***] & Ping Gao[1,2,3,9,****]

Abstract

The MYC oncoprotein activates and represses gene expression in a transcription-dependent or transcription-independent manner. Modification of mRNA emerges as a key gene expression regulatory nexus. We sought to determine whether MYC alters mRNA modifications and report here that MYC promotes cancer progression by down-regulating N6-methyladenosine (m^{6}A) preferentially in transcripts of a subset of MYC-repressed genes (MRGs). We find that MYC activates the expression of ALKBH5 and reduces m^{6}A levels in the mRNA of the selected MRGs *SPI1* and *PHF12*. We also show that MYC-regulated m^{6}A controls the translation of MRG mRNA via the specific m^{6}A reader YTHDF3. Finally, we find that inhibition of ALKBH5, or overexpression of SPI1 or PHF12, effectively suppresses the growth of MYC-deregulated B-cell lymphomas, both *in vitro* and *in vivo*. Our findings uncover a novel mechanism by which MYC suppresses gene expression by altering m^{6}A modifications in selected MRG transcripts promotes cancer progression.

Keywords ALKBH5; m^{6}A; MYC; MYC-repressed genes; oncogenesis
Subject Categories Cancer; Chromatin, Transcription & Genomics; RNA Biology
DOI 10.15252/embr.202051519 | Received 13 August 2020 | Revised 7 December 2020 | Accepted 10 December 2020 | Published online 11 January 2021
EMBO Reports (2021) 22: e51519

Introduction

MYC is critical for cell proliferation, apoptosis, differentiation, metabolism, somatic cell reprogramming, and other key processes under normal or pathological conditions, and mediates these functions by regulating numerous target genes (Fernandez *et al*, 2003; Dang, 2012; Carroll *et al*, 2018). MYC regulates up to 15% of all human genes, among which nearly one-third of the putative target genes are repressed by MYC (O'Connell *et al*, 2003; Dang *et al*, 2006; Zeller *et al*, 2006; Luscher & Vervoorts, 2012). Studies suggest that instead of regulating transcription of a new gene set, deregulated MYC functions as a transcriptional signal amplifier of extant active genes in a context-dependent manner (Lin *et al*, 2012; Nie *et al*, 2012); additional evidence also suggests that oncogenic MYC regulates gene expression selectively to promote cellular growth and cancer progression (Sabo *et al*, 2014; Walz *et al*, 2014). Despite many advances in understanding the roles of MYC, functions of MYC that are independent of canonical transcriptional regulation have not been fully evaluated.

Also, while the mechanisms whereby MYC activates transcription have been studied in considerable detail, the mode by which MYC represses gene expression is less well understood. Several mechanisms have been proposed: (i) A zinc-finger transcription factor MIZ-1 binds to initiator elements and activates transcription, whereas subsequent binding of MYC to MIZ-1 inhibits MIZ-1-mediated activation (Herkert & Eilers, 2010; Cole, 2014). (ii) Another

1 Guangzhou First People's Hospital, School of Medicine, Institutes for Life Sciences, South China University of Technology, Guangzhou, China
2 CAS Key Laboratory of Innate Immunity and Chronic Disease, Innovation Center for Cell Signaling Network, School of Life Science, University of Science and Technology of China, Hefei, Anhui, China
3 School of Biomedical Sciences and Engineering, Guangzhou International Campus, South China University of Technology, Guangzhou, China
4 Key Laboratory of Genomic and Precision Medicine, Collaborative Innovation Center of Genetics and Development, CAS Center for Excellence in Molecular Cell Science, Beijing Institute of Genomics, Chinese Academy of Sciences, Beijing, China
5 Department of Pathology, School of Medicine, Anhui Medical University, Hefei, Anhui, China
6 University of Chinese Academy of Sciences, Beijing, China
7 China National Center for Bioinformation, Beijing, China
8 Institute of Stem Cell and Regeneration, Chinese Academy of Sciences, Beijing, China
9 Guangzhou Regenerative Medicine and Health Guangdong Laboratory, Guangzhou, China
*Corresponding author. Tel: +1 617 632 4245; E-mail: gongwei_wu@dfci.harvard.edu
**Corresponding author. Tel: +86 01 82997642; E-mail: ygyang@big.ac.cn
***Corresponding author. Tel: +86 20 81048188; E-mail: eycaojie@scut.edu.cn
****Corresponding author. Tel: +86 20 39380987; E-mail: pgao2@ustc.edu.cn
†These authors contributed equally to this work
‡Present address: Department of Medical Oncology, Dana-Farber Cancer Institute, Harvard Medical School, Boston, MA, USA

mechanism, which may overlap with the first, is that MYC recruits histone deacetylases (HDACs) to a set of its target genes, and directly leads to histone deacetylation and compaction of chromatin structure to inhibit gene activation (Herkert & Eilers, 2010; Cole, 2014). (iii) Overexpression of MYC activates the histone-lysine *N*-methyltransferase EZH2 or G9a, and thereby enhances the levels of H3K27me3 or H3K9me2 on certain MYC-repressed genes, which inhibits expression of these genes (Kaur & Cole, 2013; Tu *et al*, 2018). And (iv) a critical indirect transcriptional regulation mode for MYC-mediated gene repression occurs via its ability to activate non-coding RNAs—such as microRNAs and long-non-coding RNAs—and thus repress gene expression at the protein level (Dang, 2012). However, these mechanisms explain only about 50% of MRGs; mechanisms affecting the remaining MRGs are still unknown.

N6-Methyladenosine (m^6A) is the most prevalent internal modification in mammalian mRNAs, and participates in various fundamental bioprocesses as well as cancer (Cao *et al*, 2016; Meyer & Jaffrey, 2017; Yang *et al*, 2018; Shi *et al*, 2019). Methyltransferases and demethylases, including METTL3, METTL14, ALKBH5, and FTO, are involved in the progression of certain types of cancers by regulation of m^6A modification (Lin *et al*, 2016; Zhang *et al*, 2016a; Barbieri *et al*, 2017; Zhang *et al*, 2017; Li *et al*, 2017b; Su *et al*, 2018; Weng *et al*, 2018; Lan *et al*, 2019). Whether and how MYC regulates mRNA m^6A modifications remain largely unexplored.

Here we use validated models of MYC-driven B-cell lymphoma to investigate the role of mRNA modifications in the aberrant expression of MRGs. Using integrative LC-MS, high-throughput sequencing, functional studies, and human cancer sample analyses, we document that MYC down-regulates m^6A preferentially in transcripts of certain MRGs, thereby reducing the expression of these MRGs, resulting in cancer progression. We thus unveil a novel mechanism by which MYC represses gene expression via RNA modifications during cancer progression.

Results

MYC down-regulates m^6A levels of mRNA in B-cell lymphoma cells

To investigate the effects of MYC on mRNA m^6A modification, we used the human P493-6 B-cell model of Burkitt's lymphoma (BL) (Schuhmacher *et al*, 1999; Pajic *et al*, 2000). P493-6 cells carry a MYC tetracycline (Tet)-off system, which enables the generation of cells with low or high MYC expression. To investigate whether MYC regulates mRNA m^6A levels, we determined the levels of m^6A in P493-6 cells that were treated with Tet for 72 h or 0 h. Use of a dot blot assay with purified mRNA showed that the level of mRNA m^6A modification was significantly increased when P493-6 cells were treated with Tet (Fig 1A). Our results were confirmed in the widely used BL cell line Raji, which also exhibited significantly elevated mRNA m^6A levels after knockdown of MYC with specific shRNAs (Fig 1B). The dot blot results thus indicate that MYC down-regulates total mRNA m^6A levels. This finding was verified with use of HPLC-MS, and the same samples of P493-6 cells, treated with Tet or not: We found that the m^6A/A ratio is significantly increased in the Tet-treated sample (Fig 1C). We thus conclude that loss of MYC in B-cell lymphoma cells results in increased global mRNA m^6A levels.

To identify transcriptome-wide methylation patterns regulated by MYC, we immunoprecipitated m^6A methylated poly (A^+) RNAs (MeRIP) and then sequenced and profiled mRNA m^6A methylation in P493-6 cells that were treated with Tet for 72 h or 0 h. Consistent with previous reports, mRNA m^6A peaks for both high MYC and low MYC samples were abundant in coding sequences (CDS), intron sequences, and 3′ untranslated regions (3′UTR) (Figs 1D and EV1A), and the m^6A peak was significantly enriched in GGACU/A, in both high MYC and low MYC samples (Fig EV1B). Analysis of the peak numbers and the density of m^6A peaks in both samples revealed that down-regulation of MYC resulted in higher m^6A modifications across UTRs, CDS, and introns (Figs 1D and EV1C), consistent with a global effect of MYC on gene-associated mRNA m^6A levels.

MYC preferentially down-regulates m^6A levels in mRNAs and inhibits the expression of selected MRGs

To study which genes have their m^6A methylations regulated by MYC, we used the MeRIP-seq data and identified 2,542 genes that showed significantly increased m^6A levels in low MYC samples (Fig EV1D), suggesting that MYC rewires a global m^6A modification of genes. Gene ontology (GO) term enrichment analysis revealed that this group of negative regulation of gene expression is highly enriched (Fig 1E). These genes from this enriched group are repressed by MYC, suggesting that MYC preferentially down-regulates the levels of mRNA m^6A modification of these MYC-repressed genes (MRGs). Integrative Genomics Viewer (IGV) analysis showed that m^6A peaks were increased in genes, such as B-lymphoid cell development activation transcription factor *SPI1*, SIN3A-interacting transcriptional repressor *PHF12*, Max-interacting transcriptional repressor *MXD4*, and the histone deacetylase *HDAC10* (Figs 1F and EV1E). To document whether MYC regulates m^6A modification at these genes, we purified poly (A)+ mRNA and used an m^6A antibody to perform a MeRIP assay in P493-6 cells that were treated or not with Tet. MeRIP results showed that m^6A enrichment was significantly higher at these MRG transcripts in cell samples with low MYC expression, relative to that in high MYC samples (Fig 1G). As a negative control, we found no effects on *HPRT1* (Fig 1G). These results suggest that MYC preferentially down-regulates the levels of mRNA m^6A modification of certain MRGs.

We next investigated whether MYC-regulated mRNA m^6A modification affects the expression of these MRGs. We blocked the m^6A modification by treating P493-6 cells and Raji cells with cycloleucine, a competitive inhibitor of methionine adenosyltransferase that inhibits m^6A modification (Niu *et al*, 2013), and found no changes in MYC expression over 72 h (Fig EV2A and B). Cycloleucine treatment had little effect on the mRNA expression levels of selected MRGs *SPI1* and *PHF12* (Fig EV2C) but significantly decreased their protein levels in P493-6 cells as well as Raji cells (Fig EV2A and B). The m^6A RNA immunoprecipitation (RIP) assay confirmed that cycloleucine significantly reduced mRNA m^6A levels of *SPI1* and *PHF12* (Fig EV2D). Together, these results suggest that the m^6A modification affects the protein expression of MRGs. Reduced MYC expression had no effect on mRNA levels of *SPI1* and *PHF12* (Fig EV2E) but up-regulated the protein levels of genes in both P493-6 and Raji cells (Fig 1H and I).

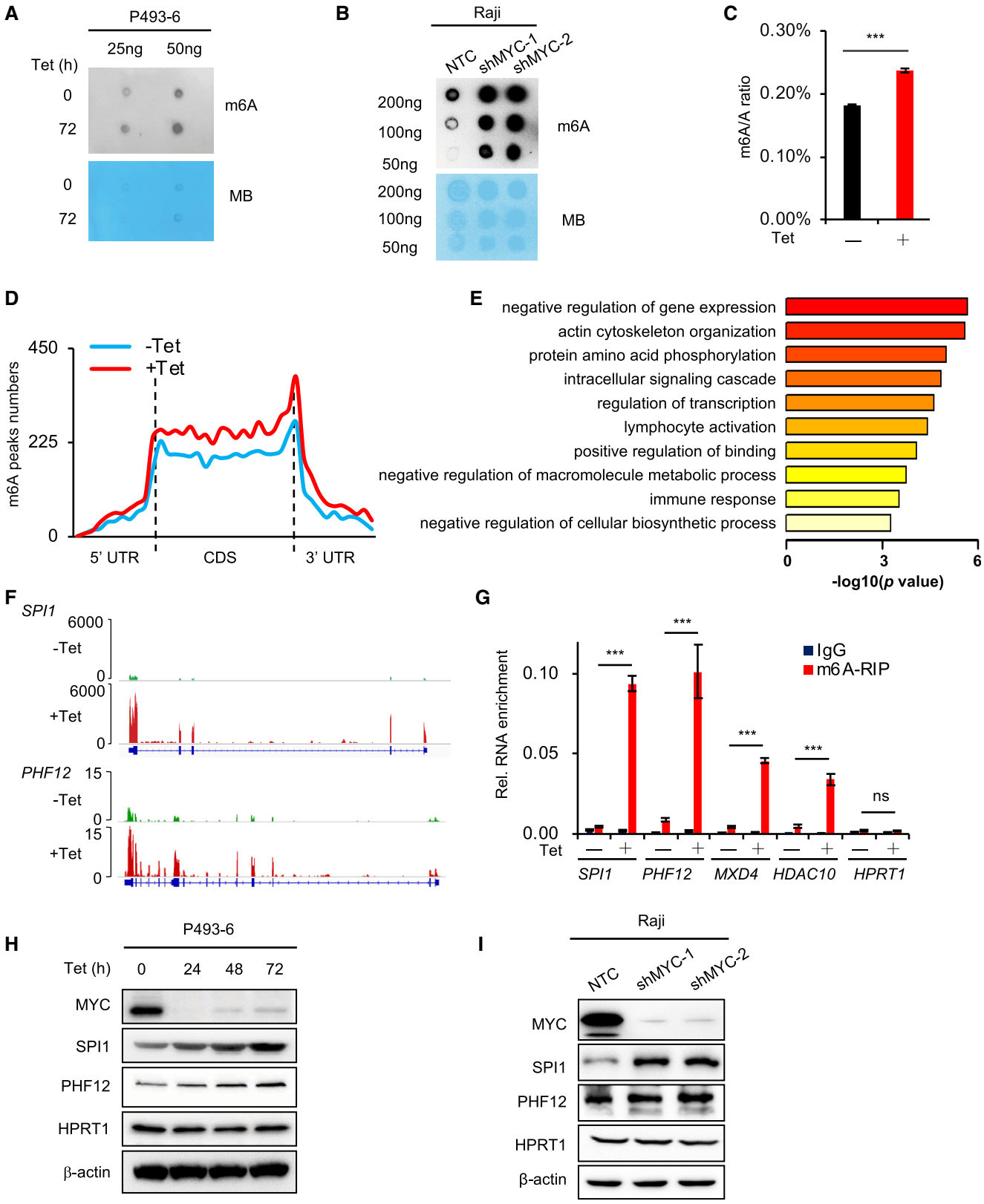
A
P493-6
25ng 50ng
Tet (h)
0
72
m6A
0
72
MB
B
Raji
NTC shMYC-1 shMYC-2
200ng
100ng
50ng
m6A
200ng
100ng
50ng
MB
C
0.30%
0.20%
0.10%
0.00%
m6A/A ratio
***
Tet
—
+
D
450
225
0
m6A peaks numbers
-Tet
+Tet
5' UTR
CDS
3' UTR
E
negative regulation of gene expression
actin cytoskeleton organization
protein amino acid phosphorylation
intracellular signaling cascade
regulation of transcription
lymphocyte activation
positive regulation of binding
negative regulation of macromolecule metabolic process
immune response
negative regulation of cellular biosynthetic process
0
3
6
-log10(p value)
F
SPI1
6000
-Tet
0
6000
+Tet
0
PHF12
15
-Tet
0
15
+Tet
0
G
IgG
m6A-RIP
Rel. RNA enrichment
0.10
0.05
0.00
Tet
***
***
***
***
ns
SPI1
PHF12
MXD4
HDAC10
HPRT1
H
P493-6
Tet (h)
0
24
48
72
MYC
SPI1
PHF12
HPRT1
β-actin
I
Raji
NTC
shMYC-1
shMYC-2
MYC
SPI1
PHF12
HPRT1
β-actin

Figure 1.

Figure 1. MYC down-regulates mRNA m^{6}A levels and inhibits protein expression of selected MRGs.

A, B m^{6}A dot blot of the P493-6 cells treated with Tet for 0 h or 72 h (A) or Raji cells that expressed NTC or *MYC* shRNAs (B); equal mRNA loading was verified by methylene blue staining. The shown data are representative of at least three independent experiments.

C Quantification of m^{6}A abundance in (A) by HPLC-MS. ***$P < 0.001$ as compared to corresponding high MYC group (mean ± SD, $n = 3$ biological replicates, Student's *t*-test).

D Metagene profiles of m^{6}A peak distribution along a normalized transcript composed of three rescaled non-overlapping segments: 5′UTR, CDS, and 3′UTR in P493-6 cells treated with Tet for 0 h or 72 h.

E Representative GO term analysis of transcripts with significantly up-regulated m^{6}A peaks in P493-6 cells treated with Tet for 72 h.

F IGV graph showing location of m^{6}A peaks on representative genes.

G m^{6}A-RIP assay in P493-6 cells treated with Tet for 0 h or 72 h. *HPRT1* serves as negative control. ***$P < 0.001$ as compared to corresponding high MYC group, ns, not significant (mean ± SD, $n = 3$ biological replicates, Student's *t*-test).

H, I Western blot analysis for protein levels in P493-6 cells treated with Tet for 0, 24, 48, and 72 h (H) or in Raji cells that expressed NTC or *MYC* shRNAs (I). HPRT1 and β-actin serve as negative and loading controls, respectively. Data are representative of at least three independent experiments.

Source data are available online for this figure.

To test whether MYC regulates the protein levels of MRGs via m^{6}A modification, we undertook a combination experiment with Tet as well as cycloleucine treatments in P493-6 cells: Tet treatment increased the protein expression of SPI1 and PHF12, but this increase was eliminated when the cells were further treated with cycloleucine (Fig EV2F). This strongly suggests that MYC regulates the protein levels of these MRGs via m^{6}A modification.

We also looked at both the m^{6}A modification and gene expression of the well-known MRGs *CDKN1A* and *CDKN2B*. IGV analysis showed that the level of m^{6}A modification of *CDKN1A* mRNA was also increased when MYC was low (Fig EV2G), suggesting the possibility that MYC regulates the gene expression of *CDKN1A* via m^{6}A modification. Of note, though there was a tiny peak at the 3′UTR region of *CDKN2B*, the m^{6}A modification level of *CDKN2B* was very low and there was no enriched m^{6}A peak for *CDKN2B* by our peak calling method (Fig EV2G), suggesting that *CDKN2B* is not an m^{6}A modification target in this context. Our RT–qPCR results showed that MYC repressed the mRNA level of *CDKN1A* and *CDKN2B* (Fig EV2H), indicating a transcriptional regulation by MYC. These data suggest that, in addition to transcriptional regulation of *CDKN1A,* MYC might also regulate the mRNA m^{6}A modification of *CDKN1A*, and MYC might regulate *CDKN2B* only by transcription.

ALKBH5 demethylates m^{6}A-modified mRNA and inhibits protein expression of selected MRGs

We next wanted to identify the enzymes responsible for regulating mRNA m^{6}A modification by MYC. We assessed the levels of the mRNA m^{6}A methyltransferases METTL3 and METTL14, and demethylases ALKBH5 and FTO in P493-6 cells and Raji cells. Tet treatment or MYC knockdown by shRNAs reduced both mRNA and protein levels of the demethylases ALKBH5 and FTO (Fig 2A–C). In contrast, there was virtually no change in the expression of the methyltransferases METTL3 or METTL14 (Fig 2A–C). Analyzing the expression of MYC, ALKBH5, and FTO in 78 lymphocyte cell lines from Cancer Cell Line Encyclopedia (CCLE) datasets and examining in various other cell lines, we found a strong correlation of MYC and ALKBH5 and FTO (Fig EV3A–C).

We analyzed the open chromatin transcription factor binding sites by chromatin immunoprecipitation sequencing (ChIP-seq) from Encyclopedia of DNA Elements (ENCODE) datasets and found the binding sites of MYC at both ALKBH5 promoter and FTO promoter (Fig EV3D). Specifically, MYC bound to the promoter regions of ALKBH5 and FTO in MCF-7 and MCF10A cells (Fig EV3E). We also analyzed published ChIP-seq datasets (Walz *et al*, 2014) and found high levels of MYC bound to the promoter regions of ALKBH5 and FTO in U2OS cells (Fig 2D). And ChIP-qPCR results in P493-6 cells showed that MYC bound to the E-box of ALKBH5 and FTO (Fig EV3F), supporting the hypothesis that MYC transcriptionally up-regulates these two demethylases.

To investigate whether ALKBH5 and FTO demethylate the mRNA m^{6}A modifications of MRG transcripts, we performed a RIP assay using antibodies against ALKBH5 and FTO. We found abundant ALBKH5 bound to the mRNA of the selected MRGs *SPI1* and *PHF12* (Fig 2E) but notably less so FTO. In Tet-treated cells, overexpression of ALKBH5 decreased protein levels of SPI1 and PHF12 (Fig 2F), without affecting mRNA levels (Fig EV3G). The effect of MYC on expression of MRG proteins was eliminated when ALKBH5 was overexpressed (Fig 2F). Also, overexpression of FTO had little or no effect on the expression of PHF12 and SPI1 (Fig 2F). Similar results were observed in Raji cells (Fig 2G).

Next, we performed an m^{6}A RIP assay in the same cells as in Fig 2F and found that when MYC was low following Tet treatment, the mRNA m^{6}A levels of MRGs *SPI1* and *PHF12* were high, and the effect of MYC on mRNA m^{6}A modification of MRGs was eliminated when ALKBH5 (but not FTO) was overexpressed (Fig 2H). To further validate whether ALKBH5 regulates mRNA m^{6}A modification and protein expression of MRGs, we performed gene knockdown experiments in P493-6 and Raji cells using *ALKBH5* shRNAs. As expected, protein but not mRNA expression of SPI1 and PHF12 was decreased in high MYC-expressing cells compared to low MYC-expressing cells (Figs 2I and J, and EV3H). These effects were reversed by knockdown of ALKBH5 (Fig 2I and J). Knockdown of ALKBH5 increased the mRNA m^{6}A levels of *SPI1* and *PHF12* and reversed the inhibitory effect of MYC on m^{6}A modification (Fig 2K). Collectively, our data demonstrate that ALKBH5 demethylates mRNA m^{6}A modifications of certain MRGs, which reduces their protein expression.

Of note, we also investigated whether ALKBH5 is involved in regulating CDKN1A and CDKN2B and detected the protein level of CDKN1A and CDKN2B in the ALKBH5 knockdown P493-6 and Raji cell samples (same to Fig 2I and J), and found that the protein level of CDKN1A was increased when knocked down ALKBH5 but not as high as in low MYC-expressing cells and CDKN2B remained the same (Fig EV3I). These data suggest that CDKN1A protein level is

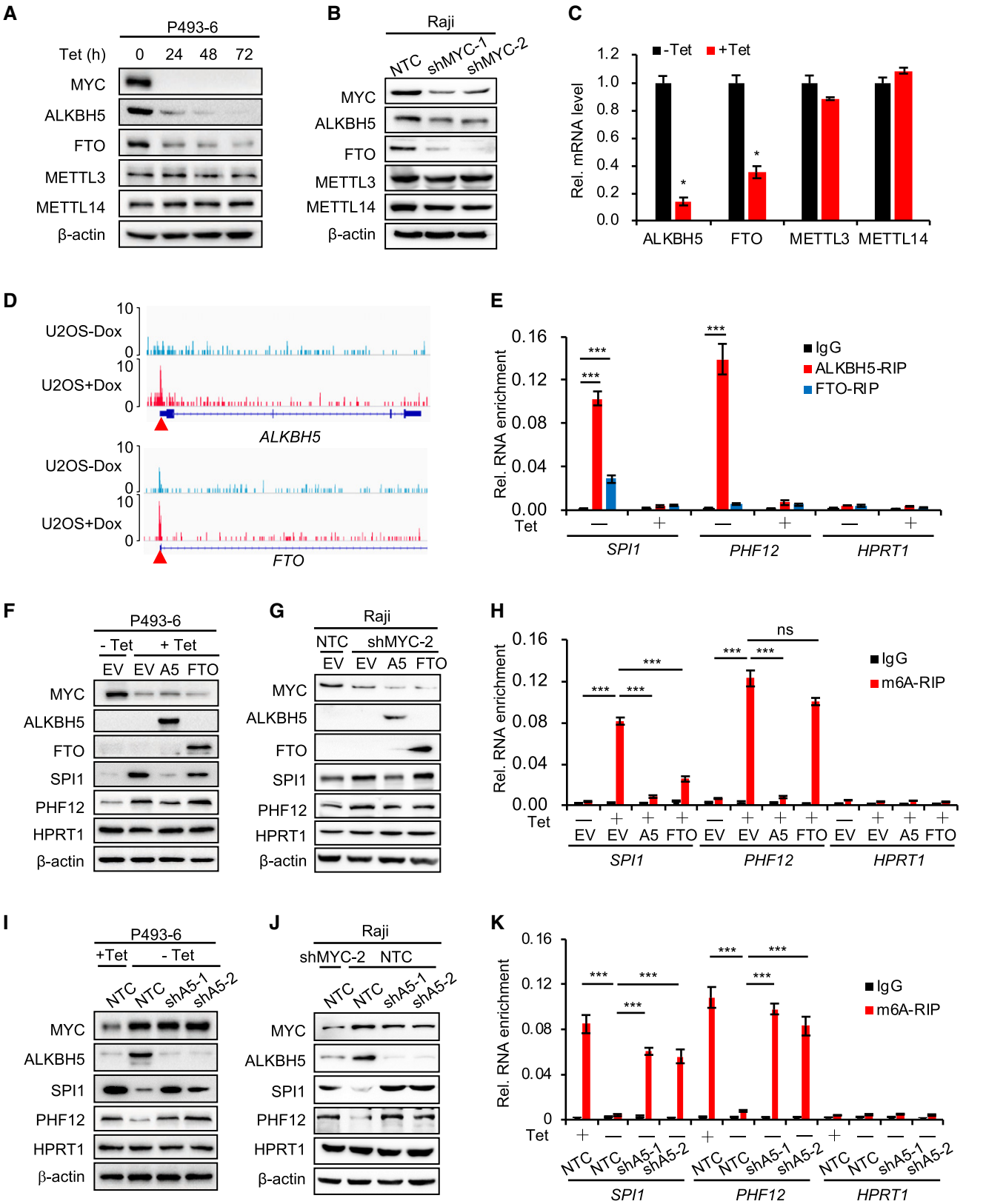
A
P493-6
Tet (h) 0 24 48 72
MYC
ALKBH5
FTO
METTL3
METTL14
β-actin
B
Raji
NTC shMYC-1 shMYC-2
MYC
ALKBH5
FTO
METTL3
METTL14
β-actin
C
-Tet +Tet
Rel. mRNA level
1.2
1.0
0.8
0.6
0.4
0.2
0.0
ALKBH5 FTO METTL3 METTL14
D
U2OS-Dox
U2OS+Dox
ALKBH5
FTO
E
Rel. RNA enrichment
IgG
ALKBH5-RIP
FTO-RIP
Tet
SPI1 PHF12 HPRT1
F
P493-6
- Tet + Tet
EV EV A5 FTO
MYC
ALKBH5
FTO
SPI1
PHF12
HPRT1
β-actin
G
Raji
NTC shMYC-2
EV EV A5 FTO
H
Rel. RNA enrichment
IgG
m6A-RIP
ns
Tet
EV EV A5 FTO EV EV A5 FTO EV EV A5 FTO
SPI1 PHF12 HPRT1
I
P493-6
+Tet - Tet
NTC NTC shA5-1 shA5-2
J
Raji
shMYC-2 NTC
K
Rel. RNA enrichment
IgG
m6A-RIP
Tet
NTC NTC shA5-1 shA5-2 NTC NTC shA5-1 shA5-2 NTC NTC shA5-1 shA5-2
SPI1 PHF12 HPRT1

Figure 2.

Figure 2. ALKBH5 removes m^{6}A from mRNA and inhibits the protein expression of SPI1/PHF12.

A, B Western blot analysis for protein levels of m^{6}A methyltransferases (METTL3 and METTL14) and demethylases (ALKBH5 and FTO) in P493-6 cells treated with Tet for 0, 24, 48, and 72 h (A) or in Raji cells that expressed NTC or *MYC* shRNAs (B). β-actin serves as loading controls. Data are representative of at least three independent experiments.

C RT–qPCR analysis of the mRNA levels of methyltransferases and demethylases in P493-6 cells treated with Tet for 0 h or 24 h. Data were presented as mean (±SD), $n = 3$ biological replicates. *$P < 0.05$ relative to corresponding -Tet group (Student's *t*-test).

D IGV graph showing location of MYC-binding peaks on *ALKBH5* and *FTO* from published ChIP-seq datasets (Data ref: Eilers, 2014; Walz *et al*, 2014). In this dataset, high levels of MYC were induced with 1 μg/ml doxycycline for 30 h and ChIPed by MYC antibody. Red triangle indicates the E-box.

E RIP assay, using ALKBH5, FTO, or IgG antibody to detect the binding to MRGs (SPI1 and PHF12) in P493-6 cells treated with Tet or not. *HPRT1* serves as negative control. ***$P < 0.001$ as compared to corresponding IgG group (mean ± SD, $n = 3$ biological replicates, Student's *t*-test).

F, G Western blot analysis for protein levels in P493-6 cells that overexpressed empty vector (EV), ALKBH5, or FTO and were then treated with Tet or not (F) or in Raji cells expressed NTC or *MYC* shRNAs (G). HPRT1 and β-actin served as negative and loading controls, respectively. Data are representative of at least three independent experiments.

H m^{6}A RIP assay in (F) that P493-6 cells that overexpressed EV, ALKBH5, or FTO and were then treated with Tet or not. *HPRT1* serves as negative control. ***$P < 0.001$ as compared between indicated groups. ns, not significant (mean ± SD, $n = 3$ biological replicates, Student's *t*-test).

I, J Western blot analysis for protein levels in P493-6 cells that expressed NTC or *ALKBH5* shRNAs and were then treated with Tet or not (I) or in Raji cells expressed NTC or *ALKBH5* shRNAs and knocked down MYC or not (J). HPRT1 and β-actin serve as negative and loading controls, respectively. Data are representative of at least three independent experiments.

K m^{6}A RIP assay in (I). *HPRT1* serves as negative control. ***$P < 0.001$ as compared between indicated groups (mean ± SD, $n = 3$ biological replicates, Student's *t*-test).

Source data are available online for this figure.

regulated by MYC via both transcriptional mechanism and m^{6}A modification. As to *CDKN2B*, MYC might regulate it only by transcription. Hence, these genes were not the focus of the subsequent studies.

YTHDF3 binds m^{6}A-modified mRNAs and facilitates translation of selected MRGs

We next asked how MYC regulates the expression of MRGs via mRNA m^{6}A methylation. YT521-B homology (YTH) domain family members are representative m^{6}A-binding proteins, and YTH m^{6}A readers are involved in m^{6}A methylation-mediated RNA fate, such as RNA stability, splicing, translation, and miRNA processing (Berlivet *et al*, 2019; Lan *et al*, 2019; Shi *et al*, 2019). We thus performed a RIP assay by using antibodies against YTH m^{6}A readers, to unveil the mechanisms that underlie regulation of MRG expression by m^{6}A modification. RIP assay results indicated that only YTHDF3 can specifically bind to the *SPI1* and *PHF12* under Tet treatment (Fig 3A), and suggested that the reader YTHDF3 binds to the MRG transcripts *SPI1* and *PHF12* and serves an important role in MYC-mediated MRG expression via m^{6}A modification. We then examined whether YTHDF3 regulates MRG protein expression. Using shRNAs that target *YTHDF3* in P493-6 cells that were treated with Tet, YTHDF3 but not YTHDF1 or YTHDF2 was significantly decreased (Fig 3B and C), and neither MYC nor YTHDF3 regulated the mRNA levels of *SPI1* and *PHF12* (Fig EV4A). However, the increase in protein levels of SPI1 and PHF12 following Tet treatment of P493-6 cells or by *MYC* shRNA in Raji cells was significantly reduced in the absence of YTHDF3 (Fig 3B and C), suggesting that MRG protein levels are up-regulated by YTHDF3.

Given that knockdown of YTHDF3 directly regulates the protein levels of MRGs (Fig 3B and C), we hypothesized that YTHDF3 regulates the translation of m^{6}A modified mRNA. To test this, we performed a polysome profiling analysis and found that such profiling of sh*YTHDF3* was much lower than in the non-targeting control (NTC) sample (Fig 3D), demonstrating that YTHDF3 regulates the translation of mRNAs. We also collected each polysome fraction, isolated the RNA, and analyzed mRNA levels of MRGs in each fraction. Our results showed that knocking down YTHDF3 significantly impaired the amount of *SPI1* and *PHF12* mRNA that bound to polysomes (Fig 3E), indicating that YTHDF3 up-regulates the translation activity of MRGs mRNA. We also performed a Click-iT AHA (L-azidohomoalanine) assay, which is used to detect the nascent proteins, to investigate whether YTHDF3 regulates the translation of these selected MRG transcripts, and found that translation of SPI1 and PHF12 was significantly decreased in the absence of YTHDF3 (Fig 3F). We thus conclude that YTHDF3 facilitates the protein translation of MRGs.

Our data have shown that MYC down-regulates the protein expression of selected MRGs by down-regulating m^{6}A modification via ALKBH5, we next investigated whether this regulatory role of m^{6}A in gene expression is YTHDF3-dependent. We analyzed MRG expression and showed that neither knocking down ALKBH5 alone nor knocking down both ALKBH5 and YTHDF3 regulates the mRNA levels of *SPI1* and *PHF12* in P493-6 cells (Fig EV4B and C). And knocking down ALKBH5 increased the protein levels of SPI1 and PHF12, but the increased protein levels were significantly attenuated when YTHDF3 was further knocked down in both P493-6 cells and Raji cells (Figs 3G and H, and EV4D), indicating that ALKBH5-mediated inhibition of MRG expression is YTHDF3-dependent. We then performed a MeRIP assay in the same cell samples as in Fig 3G. Consistently, shRNA suppression of ALKBH5 expression significantly increased m^{6}A enrichment levels (Fig 3I). And knocking down YTHDF3 did not affect the m^{6}A enrichment levels of *SPI1* and *PHF12*, eliminating the possibility that YTHDF3 regulates m^{6}A modifications (Fig 3I). Taken together, these data demonstrate that the m^{6}A reader YTHDF3 specifically binds m^{6}A and facilitates the translation of MRG transcripts.

The MYC-ALKBH5-m^{6}A-SPI1/PHF12 axis is critical for cancer progression

The above data established that MYC preferentially down-regulates the level of mRNA m^{6}A modification in mRNA of certain MRGs by

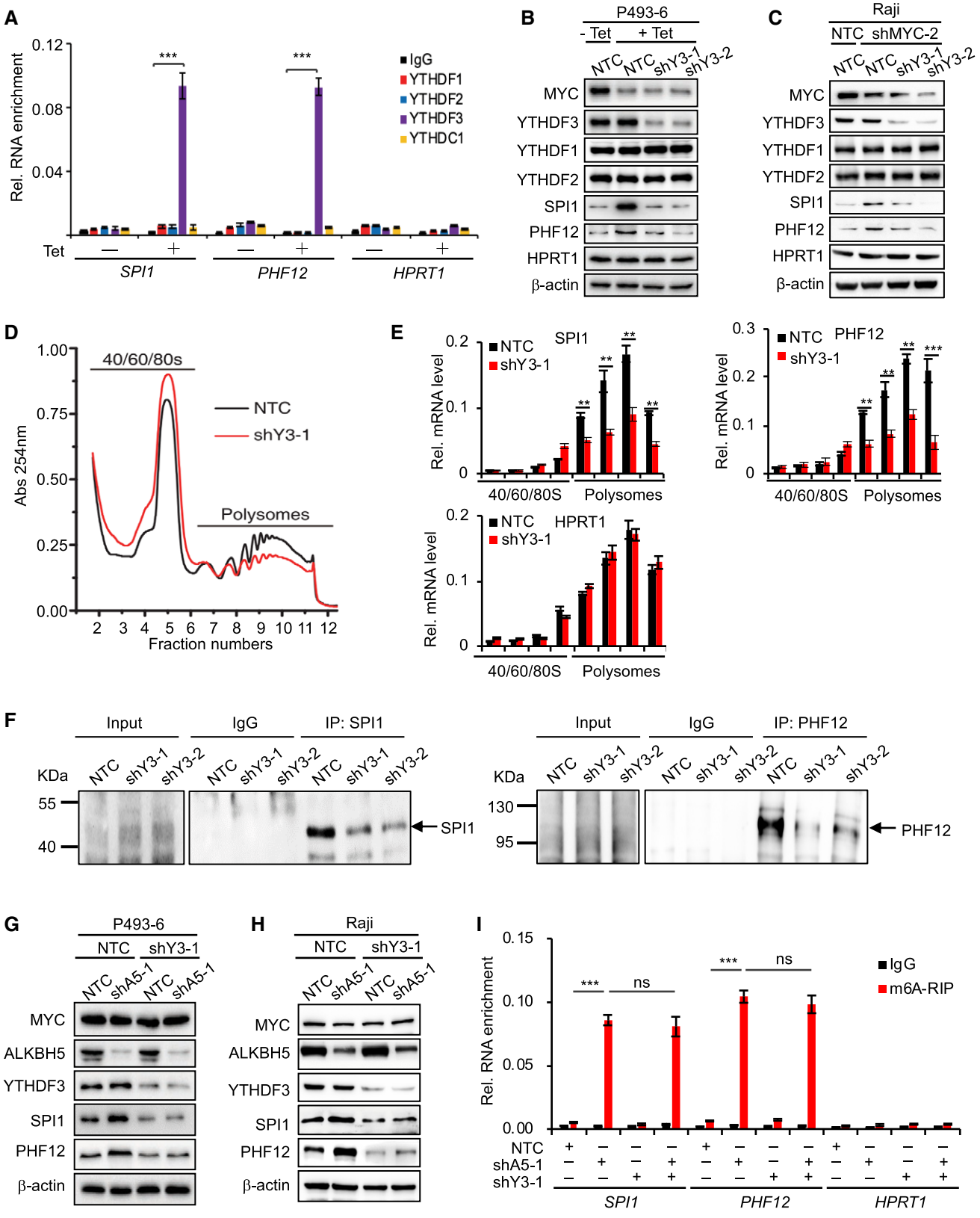
A
Rel. RNA enrichment
0.12
0.08
0.04
***
***
IgG
YTHDF1
YTHDF2
YTHDF3
YTHDC1
Tet
SPI1
PHF12
HPRT1
B
P493-6
- Tet
+ Tet
NTC
NTC
shY3-1
shY3-2
MYC
YTHDF3
YTHDF1
YTHDF2
SPI1
PHF12
HPRT1
β-actin
C
Raji
NTC
shMYC-2
NTC
NTC
shY3-1
shY3-2
MYC
YTHDF3
YTHDF1
YTHDF2
SPI1
PHF12
HPRT1
β-actin
D
Abs 254nm
1.00
0.75
0.50
0.25
0.00
40/60/80s
NTC
shY3-1
Polysomes
2 3 4 5 6 7 8 9 10 11 12
Fraction numbers
E
Rel. mRNA level
0.2
0.1
0
NTC
shY3-1
SPI1
**
**
**
**
40/60/80S
Polysomes
0.3
0.2
0.1
0
NTC
shY3-1
PHF12
**
**
**
***
40/60/80S
Polysomes
0.2
0.1
0
NTC
shY3-1
HPRT1
40/60/80S
Polysomes
F
Input
IgG
IP: SPI1
KDa
NTC
shY3-1
shY3-2
55
40
SPI1
Input
IgG
IP: PHF12
KDa
130
95
PHF12
G
P493-6
NTC
shY3-1
NTC
shA5-1
NTC
shA5-1
MYC
ALKBH5
YTHDF3
SPI1
PHF12
β-actin
H
Raji
NTC
shY3-1
NTC
shA5-1
NTC
shA5-1
MYC
ALKBH5
YTHDF3
SPI1
PHF12
β-actin
I
Rel. RNA enrichment
0.15
0.10
0.05
0.00
***
ns
***
ns
IgG
m6A-RIP
NTC
shA5-1
shY3-1
SPI1
PHF12
HPRT1

Figure 3.

Figure 3. YTHDF3 binds m^{6}A-modified mRNAs and facilitates translation of selected MRG transcripts.

A RIP assay in P493-6 cells treated with Tet for 0 h or 72 h. *HPRT1* serves as negative control. ***$P < 0.001$ relative to indicating groups (mean ± SD, $n = 3$ biological replicates, Student's *t*-test).

B, C Western blot analysis for protein levels in P493-6 cells that expressed NTC or *YTHDF3* shRNAs and were then treated with Tet or not (B) or in Raji cells that expressed NTC or *YTHDF3* shRNAs and knocked down MYC or not (C). HPRT1 and β-actin serve as negative and loading controls, respectively. Data are representative of at least three independent experiments.

D Polysomes profiling assay in P493-6 cells that expressed NTC or *YTHDF3* shRNA.

E RT–qPCR assay for mRNA levels of MRGs (*SPI1* and *PHF12*) in different fractions in (D). *HPRT1* serves as negative control. Data were presented as mean (±SD), $n = 3$ biological replicates. **$P < 0.01$ and ***$P < 0.001$ as compared to NTC group (Student's *t*-test).

F Click-iT AHA (L-azidohomoalanine) experiments were performed using IgG, anti-SPI1, or anti-PHF12 antibody. P493-6 cells expressing NTC or *YTHDF3* shRNAs were incubated for 1 h in medium containing 100 μg/ml AHA. The translated proteins were detected by Western blot. Arrow indicates translated MRGs.

G, H Western blot analysis for protein levels in P493-6 cells (G) or in Raji cells (H) that expressed NTC, or *ALKBH5* shRNA, or *YTHDF3* shRNA. β-actin serves as negative and loading controls, respectively. Data are representative of at least three independent experiments.

I m^{6}A RIP assay in (G). *HPRT1* serves as negative control. ***$P < 0.001$ as compared between indicated groups, ns, not significant (mean ± SD, $n = 3$ biological replicates, Student's *t*-test).

Source data are available online for this figure.

transcriptionally up-regulating ALKBH5, which specifically demethylates the selected MRG mRNA, then impairs the translation of these genes, and inhibits their protein expression. We next explored the effect of the MYC-ALKBH5-m^{6}A-SPI1/PHF12 axis on cell proliferation and cancer progression, and found that overexpression of ALKBH5 promotes cell proliferation in P493-6 cells (Fig EV5A) and knockdown of ALKBH5 significantly impaired cell proliferation (Fig EV5B), indicating that the MYC-regulated m^{6}A demethylase ALKBH5 is critical for cancer cell proliferation. Similar results were observed in Raji cells that knockdown of ALKBH5 alone significantly impaired cell proliferation, and overexpression of MYC promotes cell proliferation, which was eliminated when further knocking down ALKBH5 (Fig EV5C).

Deregulated MYC contributes human malignancies and therefore, we asked whether MYC promotes cancer cell proliferation by inhibiting the expression of these MRGs. We first studied the effect of MRGs on cell proliferation and found that overexpressing SPI1 or PHF12 alone significantly inhibited cell proliferation (Fig EV5D) and knocking down SPI1 or PHF12 significantly promoted cell proliferation (Fig 4A), indicating that MRGs *SPI1* and *PHF12* inhibit cancer cell proliferation and function as tumor suppressors. Also, overexpression of SPI1 or PHF12 in ALKBH5 overexpressing cells significantly suppressed the enhanced proliferation by ALKBH5 (Fig 4B and C), demonstrating that MRGs *SPI1* and *PHF12* are involved in ALKBH5-regulated cancer cell proliferation. We conclude that MYC down-regulates certain MRGs by regulating ALKBH5, and then blocks the inhibitory effect of these MRGs on cell proliferation, thereby promoting cancer cell proliferation and growth.

Given that our *in vitro* experiments show that the MYC-ALKBH5-m^{6}A-SPI1/PHF12 axis could promote cancer cell proliferation, we evaluated the effect of this axis on cancer progression *in vivo*. First, mice were xenografted with Raji cells stably expressing MYC and ALKBH5 shRNAs. Our results showed that knockdown of ALKBH5 alone significantly impaired tumor growth, and overexpression of MYC promoted tumor growth, which was eliminated by further knockdown of ALKBH5 (Fig 4D and E). Second, mice were xenografted with P493-6 cells expressing sh*SPI1* or sh*PHF12*. Our data showed that knockdown of SPI1 or PHF12 markedly accelerated tumor growth *in vivo* (Figs 4F and G, and EV5E), indicating that SPI1/PHF12 act as tumor suppressors and play an important role in tumor growth. Third, mice received a xenograft of P493-6 cells stably overexpressing ALKBH5 and MRGs: Forced expression of ALKBH5 led to a markedly accelerated tumor growth *in vivo*, and this enhanced growth was significantly suppressed by overexpression of MRGs SPI1 or PHF12 (Figs 4H and I, and EV5F). These findings are consistent with the *in vitro* data and underscore the critical role of this axis in tumor growth *in vivo*. Overexpression of ALKBH5 and MRGs was confirmed via Western blot analysis of protein lysates from xenograft tumors (Fig EV5G).

To further evaluate the physiological relevance and potential clinical significance of the MYC-ALKBH5-m^{6}A-SPI1/PHF12 regulatory axis, we used immunohistochemistry (IHC) to assess the expression of MYC, ALKBH5, SPI1, and PHF12 in samples from a retrospective cohort of 55 clinicopathologically characterized diffuse large B-cell lymphoma (DLBCL) cases and from 30 normal lymphocyte tissue samples (Li *et al*, 2020). DLBCL is the most common type of non-Hodgkin lymphoma (NHL) and is highly invasive and malignant. MYC is highly expressed in cells of this tumor and is translocated to the nucleus, which increases tumor malignancy and leads to a poor prognosis in patients with DLBCLs (Savage *et al*, 2009; Barrans *et al*, 2010; Green *et al*, 2012). As expected, DLBCLs display elevated MYC staining relative to normal lymph nodes (Fig 4J). HistoQuest software was used to analyze the mean optical density (MOD) of MYC staining for all clinical samples. A MOD cutoff of ≥ 50% defined high MYC expression, as reported (Kluk *et al*, 2012; Carey *et al*, 2015). Thus, the 55 DLBCL samples were stratified by MYC expression levels: 28 samples had low MYC expression and 27 samples had high MYC expression. The level of protein expression was determined in these two groups and also in the normal lymphocyte tissue samples: Compared to the normal samples and to the low MYC-expressing DLBCL tumor group, expression of ALKBH5 was significantly higher in the high MYC-expressing DLBCL tumors (Fig 4J). In contrast, SPI1 and PHF12 were significantly decreased in the high MYC-expressing DLBCL tumors, compared to normal samples as well as to low MYC-expressing tumors (Fig 4J). Quantitative analysis of IHC images revealed a strong positive correlation between MYC and ALKBH5, and a notable negative correlation between MYC and SPI1, as well as MYC and PHF12 (Fig 4K), underscoring the potential of the MYC-ALKBH5-SPI1/PHF12 regulatory axis as a significant prognostic pathway in DLBCL patients.

Finally, we explored the clinical and translational potential of our findings in cancers, wherein MYC is deregulated, by

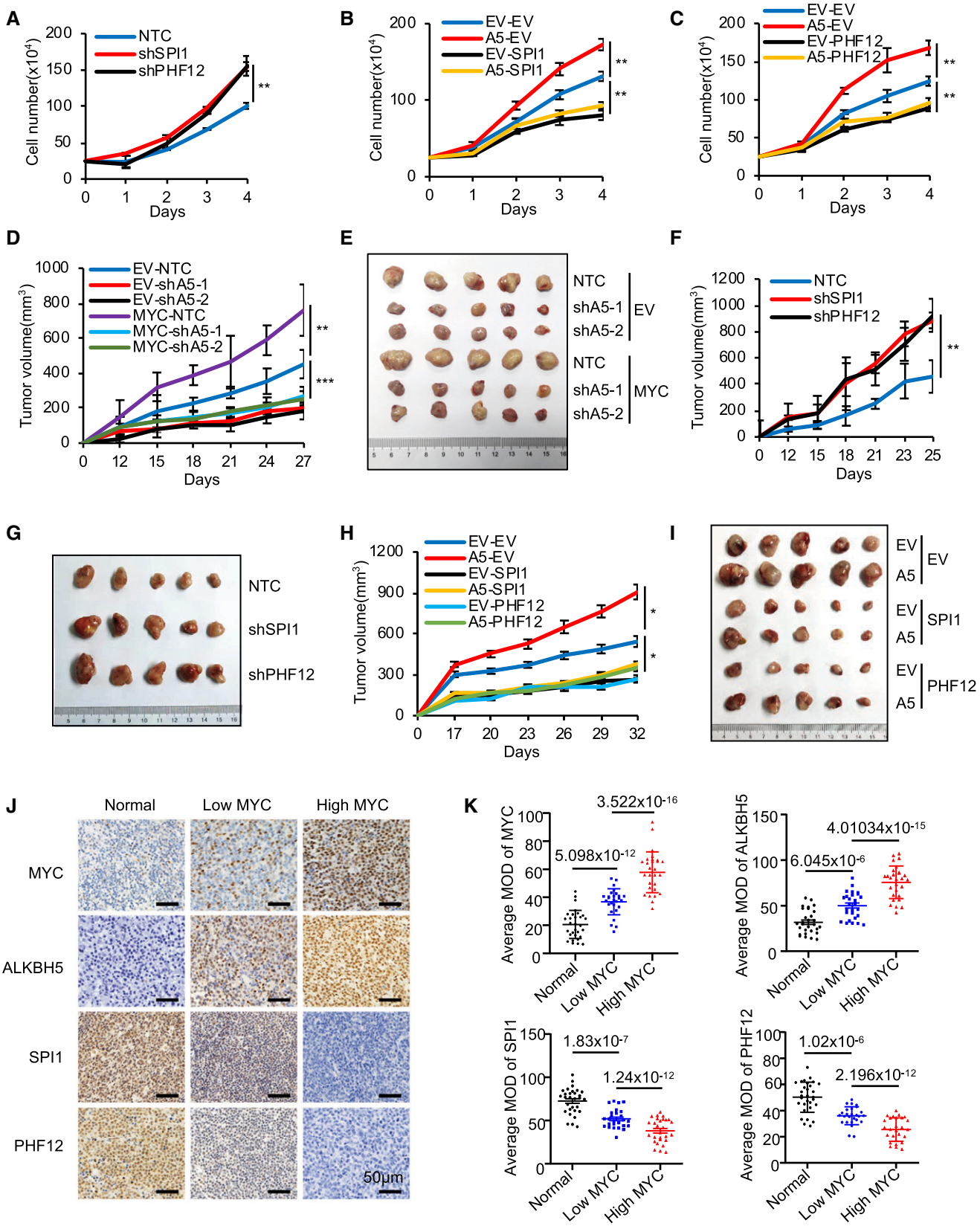
A
Cell number(x10^4)
NTC
shSPI1
shPHF12
Days
B
EV-EV
A5-EV
EV-SPI1
A5-SPI1
C
EV-EV
A5-EV
EV-PHF12
A5-PHF12
D
Tumor volume(mm^3)
EV-NTC
EV-shA5-1
EV-shA5-2
MYC-NTC
MYC-shA5-1
MYC-shA5-2
E
NTC
shA5-1
shA5-2
EV
MYC
F
G
shSPI1
shPHF12
H
I
J
Normal
Low MYC
High MYC
MYC
ALKBH5
SPI1
PHF12
50μm
K
Average MOD of MYC
3.522x10-16
5.098x10-12
Average MOD of ALKBH5
4.01034x10-15
6.045x10-6
Average MOD of SPI1
1.83x10-7
1.24x10-12
Average MOD of PHF12
1.02x10-6
2.196x10-12

Figure 4.

Figure 4. The MYC-ALKBH5-m^{6}A-SPI1/PHF12 axis is critical for cancer progression.

A Trypan blue counting was used to analyze growth curves for P493-6 cells that expressed NTC or *SPI1* shRNA or *PHF12* shRNA. $^{**}P < 0.01$ as compared between indicated groups (mean ± SD, $n = 4$ biological replicates, Student's *t*-test).

B, C Trypan blue counting was used to analyze growth curves for P493-6 cells overexpressing ALKBH5 and further infected with viruses expressing SPI1 (B) or PHF12 (C). $^{**}P < 0.01$ as compared between indicated groups (mean ± SD, $n = 4$ biological replicates, Student's *t*-test).

D, E Raji cells stably expressing EV or MYC were infected with viruses expressing sh*ALKBH5*. Cells were injected subcutaneously into nude mice ($n = 5$ for each group). Tumor growth curves were measured starting from 12 days postinjection (D). Photograph of tumors collected at the end of the experiment (day 27) (E). Data are presented as mean (±SEM). $^{**}P < 0.01$ or $^{***}P < 0.001$ as compared between indicated groups (Student's *t*-test).

F, G P493-6 cells stably expressing NTC or sh*SPI1* or sh*PHF12* were injected subcutaneously into nude mice ($n = 5$ for each group). Tumor growth curves were measured starting from 12 days postinjection (F). Photograph (G) of tumors collected at the end of the experiment (day 25). Data are presented as mean (±SEM). $^{**}P < 0.01$ as compared between indicated groups (Student's *t*-test).

H, I P493-6 cells stably expressing EV or ALKBH5 were infected with viruses expressing SPI1 or PHF12. Cells were injected subcutaneously into nude mice ($n = 5$ for each group). Tumor growth curves were measured starting from 17 days postinjection (H). Photograph (I) of tumors collected at the end of the experiment (day 32). Data are presented as mean (±SEM). $^{*}P < 0.05$ as compared between indicated groups (Student's *t*-test).

J, K Representative IHC images (J), and analysis (K) of MYC, ALKBH5, SPI1, and PHF12 expressions in normal lymphocyte tissue (normal) and lymphoma specimens. Scale bar: 50 μm. Data are presented as mean (±SEM), clinical samples $n = 30$ for normal group, $n = 28$ for low MYC expression group, and $n = 27$ for high MYC expression group; *P* value was presented between indicated groups (Student's *t*-test).

investigating whether a chemical inhibitor of m^{6}A demethylase inhibits B-cell lymphoma. We treated P493-6 cells with the ALKBH5 inhibitor IOX3 (Aik *et al*, 2014) to determine whether it affects cell proliferation and MRG expression. IOX3 treatment significantly impaired cell proliferation and increased the protein levels of SPI1 and PHF12 (Fig EV5H and I), demonstrating that IOX3 is able to inhibit MYC-deregulated cell proliferation and the regulation of ALKBH5 on MRGs. To determine whether IOX3 affects cancer progression *in vivo*, mice were xenografted with P493-6 cells and treated with or without IOX3. Our data showed that IOX3 treatment significantly impaired tumor growth *in vivo* (Fig EV5J and K), indicating that IOX3 is able to inhibit MYC-deregulated tumor growth. The results also confirm that blocking the MYC-ALKBH5-m^{6}A-SPI1/PHF12 regulatory axis with ALKBH5 inhibitor suppresses tumor growth *in vivo* and represents a promising clinical target.

Discussion

MYC-mediated gene regulation and cancer progression have been the focus of attention by many scientists and clinicians. MYC regulates up to 15% of human genes, many of which, particularly those genes which MYC represses, are not regulated via classical transcriptional regulation nor in a transcription-dependent manner (Dang *et al*, 2006; Dang, 2012; Cole, 2014; Baluapuri *et al*, 2020). We document here that MYC suppression of certain MRGs is exerted preferentially by reducing the m^{6}A modification of their transcripts and uncover a novel mechanism whereby MYC facilitates cancer progression, mainly through epigenetic modification of RNA (Fig 5). We show that treatment with IOX3, which inhibits the activity of the m^{6}A demethylase ALKBH5 and blocks the MYC-ALKBH5-m^{6}A-SPI1/PHF12 regulatory pathway, represses tumor growth *in vitro* as well as *in vivo*, unveiling a therapeutic pathway for MYC-dependent cancers.

Many efforts have been made to understand the biology of MYC oncoproteins recently. For instance, Posternak and colleagues have proposed a global role for MYC in promoting mRNA cap methylation of Wnt/β-catenin signaling genes, and in increasing their translational capacity (Posternak *et al*, 2017), while Baluapuri *et al* (2019) showed that high levels of MYC sequester SPT5 into nonfunctional complexes, and thereby decrease gene expression. However, the mechanism by which MYC directly or indirectly represses genes is not well understood (Cole & Cowling, 2008; Baluapuri *et al*, 2020). In this context, our findings elucidate a mechanism by which MYC represses genes indirectly via m^{6}A. We show that MYC down-regulates m^{6}A levels of mRNAs by activating the demethylases ALKBH5 and FTO, and thereby down-regulates mRNA m^{6}A levels of selected MRGs and inhibits their protein expression. Among these MRGs that were enriched by the GO analyses as shown in Fig 1E, considering the complexity of the genes that could be regulated by MYC at both mRNA level and m^{6}A modification level, such as *CDKN1A*, we chose those genes that are less studied and only could be regulated by MYC at m^{6}A modification level. We thus focused on *SPI1* and *PHF12* that are important in lymphomagenesis in this study. Mechanistically, by using integrative RIP and MeRIP assays, YTHDF3 knockdown experiments, polysome profiling analysis, and Click-IT AHA assay, we find that YTHDF3 specifically binds m^{6}A and facilitates the translation of *SPI1* and *PHF12* mRNA. This mechanism provides new insight into how MYC governs mRNA translation via the mRNA m^{6}A modification, in addition to the known mechanisms that involve stimulation of ribosome biogenesis, tRNA synthesis, transcription of genes that encode translation factors, and interacting with RNA-binding proteins (Cole & Cowling, 2008; Cargnello & Topisirovic, 2019; Singh *et al*, 2019).

Analyses of mouse models and clinical samples reveal that MRGs play an essential role in MYC-deregulated cancers. The sample analyses document that SPI1 and PHF12 are highly expressed in normal tissue, relative to tumor tissue in which cells exhibit high MYC expression (Fig 4J and K). Our *in vitro* and *in vivo* experiments demonstrate that overexpression of SPI1 or PHF12 impairs cancer progression (Figs 4B, C, H, I, and EV5D and F) and that knocking down SPI1 or PHF12 significantly accelerates cancer progression (Figs 4A, F, G, and EV5E). These observations indicate not only that MYC activated genes, but also these MRGs—which are not very well studied—make important contributions to the normal development as well as to many oncogenic functions of MYC. Based on these findings, we suggest that when MYC is low, m^{6}A levels of certain MRG transcripts are high, which facilitates their and leads to cell proliferation and growth inhibition under the control of the MRGs. Conversely, when MYC is overexpressed, m^{6}A levels of MRG transcripts are reduced, which reduces protein expressions of MRGs,

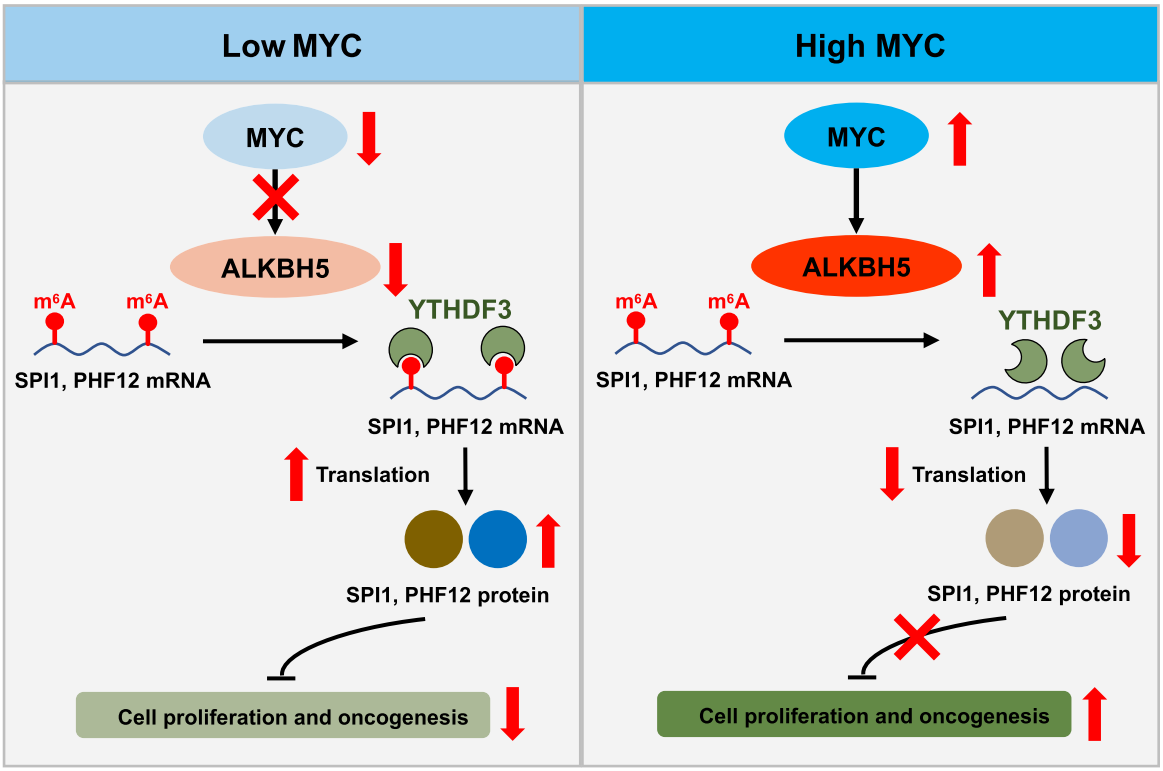

Figure 5. Working model: MYC suppression of gene expression via m^{6}A is critical for cancer progression.

MYC down-regulates the m^{6}A modification preferentially in certain MRGs, by up-regulating the demethylase ALKBH5. The m^{6}A reader YTHDF3-mediated translation of MRGs SPI1 and PHF12 is attenuated as decreased m^{6}A modification, and thus releases the inhibitory effect of MRGs on cell proliferation, thereby promoting cancer progression. The up-direction red arrows indicate high, and down-direction red arrows indicate low.

and in turn triggers uncontrolled cell growth. Additional studies of various MYC-deregulated tumor mouse models and of clinical cancer samples will enable us to more fully elucidate the importance of MYC, m^{6}A, and MRGs, and how they are associated with the development of cancers, by tracking m^{6}A levels and MRG expression.

Since the first m^{6}A modification enzyme FTO was discovered in 2011, interest in mRNA m^{6}A modifications has increased greatly: Many m^{6}A modification-related enzymes have been reported, and m^{6}A modifications are now known to participate in a number of fundamental biological processes. Emerging evidence suggests m^{6}A also plays an important role in malignancy (Bansal *et al*, 2014; Li *et al*, 2017b; Nishizawa *et al*, 2018; Su *et al*, 2018; Weng *et al*, 2018; Cheng *et al*, 2019; Lan *et al*, 2019). Several reports claim that MYC is a target of the m^{6}A methyltransferases METTL3 and METTL14, and that the mRNA m^{6}A modification of MYC is regulated by METTL3 or METTL14 in some cancers (Lin *et al*, 2016; Su *et al*, 2018; Weng *et al*, 2018; Cheng *et al*, 2019), implicating MYC and m^{6}A in cancer. Here, we have examined whether MYC regulates mRNA m^{6}A modifications, investigated the underlying mechanisms, and reported on the consequences for cancer progression. We conclude that MYC down-regulates mRNA m^{6}A levels. Unlike the methyltransferases METTL3 and METTL14, which regulate the mRNA m^{6}A level of MYC, MYC itself regulates the expression of the demethylases ALKBH5 and FTO. Further, RIP and MeRIP assays show that ALKBH5 specifically demethylates the mRNA m^{6}A levels of certain MRG transcripts. Moreover, consistent with previous findings, the m^{6}A reader YTHDF3 facilitates mRNA translation (Shi *et al*, 2017; Li *et al*, 2017a), thus promoting protein expression of MRGs. Finally, the *in vitro* and *in vivo* experiments show that the MYC-ALKBH5-m^{6}A-SPI1/PHF12 regulatory axis is critical for MYC-deregulated cancer progression, and that inhibition of ALKBH5 with IOX3 or knockdown of ALKBH5 with shRNAs significantly impairs cancer progression. This is consistent with reports from several other groups that knocking down ALKBH5 with shRNAs decreases cancer progression (Zhang *et al*, 2016a; Zhang *et al*, 2016b; Zhang *et al*, 2017). Of note, there is no ALKBH5-specific inhibitor currently available and IOX3 that we used here might have other potential targets. Another limitation of this study is that we were able to explore only a small subset of MRGs in detail; thus, it is possible that the other MRG transcripts are regulated by FTO, which is reportedly related to obesity and cancers (Lin *et al*, 2016; Li *et al*, 2017b; Su *et al*, 2018; Huang *et al*, 2019; Yang *et al*, 2019; Melstrom & Chen, 2020). Targeting FTO with the specific inhibitor FB23-2 significantly inhibits AML progression (Huang *et al*, 2019), suggesting that FTO might be another potential target for MYC-deregulated cancer. Together, we show that targeting ALKBH5 and blocking the MYC-ALKBH5-m^{6}A-SPI1/PHF12 regulatory pathway represses tumor growth *in vitro* as well as *in vivo*, unveiling a therapeutic potential of m^{6}A demethylases for MYC-dependent cancers.

Overall, our work reveals a novel regulatory pathway downstream of MYC regulating gene expression by showing global

alterations of m^6A levels. Specifically, we show that the oncogene MYC down-regulates the m^6A level of mRNA by activating demethylases and preferentially down-regulates the expression of certain MRGs via mRNA m^6A modifications. We document that not only does MYC down-regulate the m^6A levels of mRNAs in cancer cells, but we also unveil a novel mechanism where MYC suppresses of gene expression via m^6A modifications, providing new insights into how MRGs are regulated. The MYC-ALKBH5-m^6A-SPI1/PHF12 regulatory axis that we have identified here is critical for cancer progression and may represent a promising clinical target for human malignancies with aberrant MYC expression.

Materials and Methods

Cell culture and reagents

HEK293T cells (from ATCC) were cultured in Dulbecco's modified Eagle medium DMEM (Gibco) with 10% FBS (Gibco). P493-6 B cells (gift of Dr. Chi V. Dang at Ludwig Institute for Cancer Research) were cultured in RPMI-1640 (Gibco) with 10% Tet system approved FBS (Takara Bio). Raji cells (from the Type Culture Collection of Chinese Academy of Sciences, Shanghai, China) were cultured in RPMI-1640 medium (Gibco) with 10% FBS (Gibco). All cell lines were tested for and found to be free of mycoplasma contamination. DMEM and RPMI-1640 were supplemented with 1% penicillin–streptomycin (Gibco). Cells were maintained in 5% CO_2 at 37°C. To repress MYC expression in P493-6 B cells, 0.1 μg/ml tetracycline (Sigma-Aldrich, T7660) was added to the culture medium. Chemical m^6A inhibition was achieved with use of 20 mM cycloleucine (Sigma-Aldrich, A48105). ALKBH5 inhibitor IOX3 was purchased from Selleckchem (Catalog No. S7979).

Plasmids and established stable cells

pCDH-EV empty vector or pCDH-SPI1, pCDH-PHF12/pSin-3XFlag-EV, pSin-3XFlag-ALKBH5, pSin-3XFlag-FTO vectors were co-transfected with plasmids encoding Δ8.9 and VSVG, into HEK293T packaging cells, using lipofectamine 2000 (Invitrogen). P493-6 B cells were infected with produced lentivirus in the presence of polybrene, and selected with 0.5 μg/ml puromycin, to establish stable cells. Lentiviral shRNAs targeting human *MYC*, *ALKBH5*, *YTHDF3*, *SPI1*, or *PHF12* were purchased from Sigma (targeting sequences listed in Table EV1). Virus-expressing shRNAs were produced in HEK293T cells and transduced into P493-6 B cells and Raji cells in the presence of polybrene.

RNA extraction and quantitative real-time PCR

Total RNA was isolated using TRIzol reagent (Life technologies) and treated with DNase (Ambion). One microgram of RNA was used to synthesize cDNA, employing the iScriptcDNA Synthesis Kit (Bio-Rad) (sequences of used primers shown in Table EV2). Quantitative real-time PCR was performed using iQ SYBR Green Supermix and the iCycler Real-time PCR Detection System (Bio-Rad). mRNA levels were compared to 18S rRNA or RPL13A, and the fold change of target mRNA expression was calculated based on a threshold cycle (Ct), where $\Delta Ct = Ct_{\text{target}} - Ct_{18S}$ and $\Delta(\Delta Ct) = \Delta Ct_{\text{Control}} - \Delta Ct_{\text{Indicated condition}}$.

Western blotting

Proteins were extracted using RIPA buffer (50 mM Tris–HCl, pH 8.0, 150 mM NaCl, 5 mM EDTA, 0.1% SDS, 1% NP-40), supplemented with a protease inhibitor cocktail, and quantified with a Bradford assay kit (Sangon Bio). Equal amounts of protein were fractionated by 5–12% SDS–PAGE. The following primary antibodies were used: METTL14 (1:1,000, HPA038002), ALKBH5 (1:1,000, HPA007196) (Sigma-Aldrich, St Louis, MO, USA); YTHDC1 (1:1,000, ab122340), FTO (1:1,000, ab124892) (Abcam, Cambridge, USA); MYC (1:2,000, 9402s), SPI1 (1:1,000, 2258s) (Cell Signaling Technology, Beverly, MA, USA); METTL3 (1:1,000, 15073-1-AP), YTHDF1 (1:1,000, 17479-1-AP), YTHDF2 (1:1,000, 24744-1-AP), YTHDF3 (1:1,000, 25537-1-AP), PHF12 (1:1,000, 24485-1-AP), HPRT1 (1:1,000, 15059-1-AP), CDKN1A (1:1,000, 10355-1-AP), CDKN2B (1:1,000, 12877-1-AP), β-actin (1:5,000, 66009-1-Ig) (Proteintech, Rosemont, IL, USA). HRP-conjugated anti-rabbit and anti-mouse (1:10,000, Bio-Rad) secondary antibodies were used. Signaling was detected by Western ECL Substrate (Bio-Rad).

Click-iT AHA (L-azidohomoalanine)

For the Click-iT AHA analysis, P493-6 cells were washed with PBS twice and then incubated in DMEM supplemented with or without methionine, cysteine for 1 h, followed by culturing in DMEM supplied with 100 μg/ml AHA (C10102; Invitrogen) plus 10% FBS, for 1 h in 5% CO_2 at 37°C. Cells were lysed with IP buffer (1% NP-40, 20 mM HEPES (pH 7.4), 150 mM NaCl, 2 mM EDTA, 1.5 mM $MaCl_2$) supplemented with a protease inhibitor cocktail for 45 min on ice, followed by centrifugation at 16,000 *g* for 10 min at 4°C. Supernatants were incubated with the indicated antibodies for 4 h at 4°C and then with protein A/G-conjugated beads for 2 h. Beads were washed five times with IP buffer. Eluted samples were incubated with 40 μM Biotin-PEG4-Alkyne for 30 min in Click-iT Protein Reaction Buffer (C10276; Invitrogen) following the manufacturer's protocol. The proteins were extracted with methanol and chloroform and analyzed by Western blot using streptavidin-conjugated horseradish peroxidase.

Polysome profiling analysis

P493-6 cells were treated with a final concentration of 100 μg/ml cycloheximide (Sigma-Aldrich) for 5 min. Cells were washed 2× in 10 ml of ice-cold PBS containing 100 μg/ml cycloheximide and lysed in lysis buffer (5 mM Tris–HCl (pH 7.5), 2.5 mM $MgCl_2$, 1.5 mM KCl, 0.1 mg/ml cycloheximide, 10 mM DTT, 0.5% Triton X-100, 0.5% sodium deoxycholate) supplemented with a protease inhibitor cocktail (EDTA-free) plus the RNase inhibitor RNasin (Promega), and centrifuged at 21,000 *g* for 5 min at 4°C. Supernatants were quantified by NanoDrop, and same OD amount of lysate was loaded onto each gradient. Each gradient was centrifuged at 164,000 *g* for 2 h at 4°C using the SW40Ti rotor in a Beckman Coulter ultracentrifuge. Each tube was screwed onto the ISCO UV detector, and the chasing solution was run through the gradient. Data were collected with use of the TracerDAQ program and fractions collected over time. RNA was isolated from each fraction and detected by RT–qPCR.

Chromatin immunoprecipitation

The ChIP assay was performed as described (Wu *et al*, 2017) with use of an EZ-ChIP kit (Millipuro), according to the manufacturer's instructions. Briefly, cells were fixed with 1% formaldehyde, quenched in 0.125 M glycine, and sonicated in a Bioruptor Sonication System UCD-300. DNA was immunoprecipitated with use of control IgG or a primary antibody against MYC (Cell Signaling Technology, 9402s), followed by RT–qPCR analysis (Bio-Rad). Oligos used for this analysis are listed in Table EV2.

m^{6}A dot blot assay

Immediately after harvesting the cells, total RNA was isolated using Trizol (Invitrogen, 15596-018, as per the manufacturer's instructions) and purified with the Dynabeads® mRNA purification kit (Ambion, 61006) for two rounds. Isolated mRNA was first denatured by heating at 95°C for 3 min, followed by chilling on ice. RNA samples were quantified using NanoDrop. Twofold serial dilutions were spotted on an Amersham Hybond-N + membrane, which was optimized for nucleic acid transfer (GE Healthcare). After UV crosslinking in a Stratagene Stratalinker 2400 UV Crosslinker, the membrane was washed with PBST buffer, blocked in 5% non-fat milk in PBST, incubated with anti-m^{6}A antibody (1:2,000; Synaptic Systems) overnight at 4°C, and incubated with HRP-conjugated anti-rabbit IgG secondary antibody and detected by an ECL Western Blotting Detection Kit (Bio-Rad). To verify that equal amounts of mRNA were spotted on the membrane, the blot was stained with 0.02% methylene blue in 0.3 M sodium acetate (pH 5.2).

RNA immunoprecipitation

Cells were collected, pelleted by centrifuge for 5 min at 600 *g*, and washed twice with cold PBS. The cell pellet was re-suspended with 1 ml of lysis buffer (150 mM KCl, 10 mM HEPES pH 7.6, 2 mM EDTA, 0.5% NP-40, 0.5 mM DTT, 1:100 protease inhibitor cocktail, 400 U/ml RNase inhibitor), and then the messenger ribonucleoprotein (mRNP) lysate was incubated on ice for 30 min and shock-frozen at −80°C with liquid nitrogen. The mRNP lysate was thawed on ice and centrifuged at 15,000 *g* for 15 min to clear the lysate. Cell lysate was pre-cleared with 40 µl protein A/G beads. 50 µl of pre-cleared lysate was saved as input, mixed with 50 µl TRIzol, and stored at −80°C. Protein A/G beads were coated with indicated antibody (2 µg) or IgG control antibody for 2 h at 4°C. Then, the antibody-coated beads were mixed with pre-cleared cell lysate and incubated overnight at 4°C. mRNP bound to protein A/G beads was washed 6 times with washing buffer (200 mM NaCl, 50 mM HEPES pH 7.6, 2 mM EDTA, 0.05% NP-40, 0.5 mM DTT, 200 U/ml RNase inhibitor), and RNA was extracted with 500 µl TRIzol.

m^{6}A immunoprecipitation

Total RNAs were extracted with TRNzol (Invitrogen, 15596-018) and then purified with the Dynabeads® mRNA purification kit (Ambion, 61006) for two rounds. For detecting levels of m^{6}A, the purified mRNAs were analyzed through UHPLC-MS/MS as described (Jia *et al*, 2011).

To immunoprecipitated m^{6}A, purified mRNAs were digested by DNase I and then incubated at 94°C for 30 s in fragmentation buffer (10 mM $ZnCl_2$, 10 mM Tris–HCl, pH 7.0), to cut them into pieces of ~ 300-nt. The reaction was stopped with 0.05 M EDTA (Ambion, AM8740) and was followed by standard ethanol precipitation and collection. Anti-m^{6}A polyclonal antibody (12 µg antibody for 6 µg mRNAs; Synaptic Systems, 202003) was incubated with 50 µl protein A beads (Sigma, P9424) in IPP buffer (150 mM NaCl, 0.1% NP-40, 10 mM Tris–HCl, pH 7.4) for 1 h at room temperature. The mRNAs (6 µg) were incubated with the prepared antibody-beads mixture for 4 h at 4°C. After washing, bound RNAs were extracted by TRNzol and reverse-transcribed, and then amplified by PCR. Enrichment of m^{6}A was quantified using RT–qPCR. Sequences of the qPCR primers are listed in Table EV2.

MeRIP-seq and data analysis

MeRIP was performed as above, except that RNA was cut into fragments of ~ 100-nt. An Illumina HiSeq 2000 platform was used for the MeRIP sequencing; reads were mapped to the UCSC human genome hg19 using TopHat (version 2.0.9). Only unique mapped reads with mapping quality more than or equal to 20 were kept for the subsequent analysis for each sample. The m^{6}A-enriched regions in each MeRIP sample were extracted using MACS2 software (version 2.0.10), with the corresponding input sample serving as control. Motifs were analyzed by HOMER (Hypergeometric Optimization of Motif EnRichment) (version 3.12). Gene traces were visualized using the Integrative Genomics Viewer. Original data are available in NCBI GEO (accession number GSE150892).

Animal studies

All animal studies were approved by the Animal Research Ethics Committee of the South China University of Technology. For xenograft experiments, 2×10^7 P493-6 cells or 1×10^7 Raji cells were injected subcutaneously into 6-week-old male BALb/c nude mice ($n = 5$ for each group) (SJA Laboratory Animal Company, China); starting at 10 days postinjection, tumors were measured every 2 or 3 days with a caliper and volumes were calculated using the equation: volume = width*depth*length*0.5. IOX3 was dissolved first in dimethylsulfoxide (DMSO) and then in sterile H_2O (pH 7.0) (5% DMSO/H_2O). A single dose of IOX3 (15 mg/kg) or vehicle (5% DMSO/H_2O) was given to mice through intragastric administration every other day.

Clinical human tissue specimen and immunohistochemistry

Formalin-fixed, paraffin-embedded primary DLBCLs and normal lymph node specimens obtained from 85 patients were randomly selected from the archives of the First Affiliated Hospital of Anhui Medical University. To use these clinical materials for research purposes, written informed consent from patients and approval from the Institutional Research Ethics Committee of the First Affiliated Hospital of Anhui Medical University were obtained. Immunohistochemistry (IHC) was performed as described (Li *et al*, 2020). Images were acquired with a Zeiss AxioImager Z1 and quantified with HistoQuest (Tissue Gnostics GmbH, Vienna, Austria, www.tissuegnostics.com). Images of ten zones (X200 objective) in each

sample were analyzed, to verify the mean optical density (MOD); data were statistically analyzed by a *t*-test. Exposure time, signal amplification, and objectives were the same for all samples when obtaining images. Primary antibodies against the following proteins were used for IHC: MYC (ZA0555, ZSGB-BIO), ALKBH5 (HPA007196, Sigma-Aldrich), SPI1 (2258s, Cell Signaling Technology), PHF12 (PA5-48127, Thermo Fisher Scientific).

Statistical analyses

Clinicopathological characteristics were analyzed by the chi-square test. Statistical analysis was determined using Student's *t*-test for other experiments. Differences were considered to be statistically significant at the $P < 0.05$ level ($*P < 0.05$, $**P < 0.01$, $***P < 0.001$, $****P < 0.0001$, n.s. not significant). Error bars represent SD or SEM.

Data availability

The data that support the findings of this study are available from the corresponding author on reasonable request. The MeRIP-seq datasets reported in this study are available in the NCBI Gene Expression Omnibus GSE150892 (https://www.ncbi.nlm.nih.gov/geo/query/acc.cgi?acc=GSE150892).

Expanded View for this article is available online.

Acknowledgements
We thank Drs. David M Weinstock and Sonal Jhaveri at Dana-Farber Cancer Institute for critical reading of this manuscript and valuable suggestions. This work is supported in part by National Key R&D Program of China (2018YFA0800300, 2018YFA0107103), National Natural Science Foundation of China (91957203, 81525022, 81930083, 31571472, 81530076, 81821001, 31625016, 81874060), the Chinese Academy of Sciences (XDB39020100), the Program for Guangdong Introducing Innovative and Entrepreneurial Teams (2017ZT07S054), and Outstanding Scholar Program of Guangzhou Regenerative Medicine and Health Guangdong Laboratory (2018GZR110102001), The K. C. Wong Education Foundation, Shanghai Municipal Science and Technology Major Project (2017SHZDZX01).

Author contributions
PG, GW, Y-GY, and JC conceived this study. GW, CS, LS, HZ, and PG designed the experiments. GW, CS, YY, YZ, S-TL, DY, YW, YC, and NW executed the experiments. SS and YY analyzed MeRIP sequencing data. GW, CS, and PG wrote the manuscript. All the authors analyzed the results, read, and approved the manuscript.

Conflict of interest
The authors declare that they have no conflict of interest.

References

Aik W, Scotti JS, Choi H, Gong L, Demetriades M, Schofield CJ, McDonough MA (2014) Structure of human RNA N(6)-methyladenine demethylase ALKBH5 provides insights into its mechanisms of nucleic acid recognition and demethylation. *Nucleic Acids Res* 42: 4741 – 4754

Baluapuri A, Hofstetter J, Dudvarski Stankovic N, Endres T, Bhandare P, Vos SM, Adhikari B, Schwarz JD, Narain A, Vogt M *et al* (2019) MYC Recruits SPT5 to RNA polymerase II to promote processive transcription elongation. *Mol Cell* 74: 674 – 687

Baluapuri A, Wolf E, Eilers M (2020) Target gene-independent functions of MYC oncoproteins. *Nat Rev Mol Cell Biol* 21: 255 – 267

Bansal H, Yihua Q, Iyer SP, Ganapathy S, Proia DA, Penalva LO, Uren PJ, Suresh U, Carew JS, Karnad AB *et al* (2014) WTAP is a novel oncogenic protein in acute myeloid leukemia. *Leukemia* 28: 1171 – 1174

Barbieri I, Tzelepis K, Pandolfini L, Shi J, Millan-Zambrano G, Robson SC, Aspris D, Migliori V, Bannister AJ, Han N *et al* (2017) Promoter-bound METTL3 maintains myeloid leukaemia by m(6)A-dependent translation control. *Nature* 552: 126 – 131

Barrans S, Crouch S, Smith A, Turner K, Owen R, Patmore R, Roman E, Jack A (2010) Rearrangement of MYC is associated with poor prognosis in patients with diffuse large B-cell lymphoma treated in the era of rituximab. *J Clin Oncol* 28: 3360 – 3365

Berlivet S, Scutenaire J, Deragon JM, Bousquet-Antonelli C (2019) Readers of the m(6)A epitranscriptomic code. *Biochim Biophys Acta Gene Regul Mech* 1862: 329 – 342

Cao G, Li HB, Yin Z, Flavell RA (2016) Recent advances in dynamic m6A RNA modification. *Open Biol* 6: 160003

Carey CD, Gusenleitner D, Chapuy B, Kovach AE, Kluk MJ, Sun HH, Crossland RE, Bacon CM, Rand V, Dal Cin P *et al* (2015) Molecular classification of MYC-driven B-cell lymphomas by targeted gene expression profiling of fixed biopsy specimens. *J Mol Diagn* 17: 19 – 30

Cargnello M, Topisirovic I (2019) c-Myc steers translation in lymphoma. *J Exp Med* 216: 1471 – 1473

Carroll PA, Freie BW, Mathsyaraja H, Eisenman RN (2018) The MYC transcription factor network: balancing metabolism, proliferation and oncogenesis. *Front Med* 12: 412 – 425

Cheng M, Sheng L, Gao Q, Xiong Q, Zhang H, Wu M, Liang Y, Zhu F, Zhang Y, Zhang X *et al* (2019) The m(6)A methyltransferase METTL3 promotes bladder cancer progression via AFF4/NF-kappaB/MYC signaling network. *Oncogene* 38: 3667 – 3680

Cole MD, Cowling VH (2008) Transcription-independent functions of MYC: regulation of translation and DNA replication. *Nat Rev Mol Cell Biol* 9: 810 – 815

Cole MD (2014) MYC association with cancer risk and a new model of MYC-mediated repression. *Cold Spring Harb Perspect Med* 4: a014316

Dang CV, O'Donnell KA, Zeller KI, Nguyen T, Osthus RC, Li F (2006) The c-Myc target gene network. *Semin Cancer Biol* 16: 253 – 264

Dang CV (2012) MYC on the path to cancer. *Cell* 149: 22 – 35

Eilers M (2014) Gene Expression Omnibus GSM1231597 (https://www.ncbi.nlm.nih.gov/geo/query/acc.cgi?acc=GSM1231597). [DATASET]

Fernandez PC, Frank SR, Wang L, Schroeder M, Liu S, Greene J, Cocito A, Amati B (2003) Genomic targets of the human c-Myc protein. *Genes Dev* 17: 1115 – 1129

Furey T, Zhang Z, Song L, Crawford G, Giresi P, Lieb J, Liu Z, McDaniell R, Lee B, Iyer V *et al* (2011) Gene Expression Omnibus GSE33213 (https://www.ncbi.nlm.nih.gov/geo/query/acc.cgi?acc=GSE33213) [DATASET]

Green TM, Nielsen O, de Stricker K, Xu-Monette ZY, Young KH, Moller MB (2012) High levels of nuclear MYC protein predict the presence of MYC rearrangement in diffuse large B-cell lymphoma. *Am J Surg Pathol* 36: 612 – 619

Herkert B, Eilers M (2010) Transcriptional repression: the dark side of myc. *Genes Cancer* 1: 580 – 586

Huang Y, Su R, Sheng Y, Dong L, Dong Z, Xu H, Ni T, Zhang ZS, Zhang T, Li C *et al* (2019) Small-molecule targeting of oncogenic FTO demethylase in acute myeloid leukemia. *Cancer Cell* 35: 677 – 691

Jia G, Fu Y, Zhao X, Dai Q, Zheng G, Yang Y, Yi C, Lindahl T, Pan T, Yang YG *et al* (2011) N6-methyladenosine in nuclear RNA is a major substrate of the obesity-associated FTO. *Nat Chem Biol* 7: 885 – 887

Kaur M, Cole MD (2013) MYC acts via the PTEN tumor suppressor to elicit autoregulation and genome-wide gene repression by activation of the Ezh2 methyltransferase. *Cancer Res* 73: 695 – 705

Kluk MJ, Chapuy B, Sinha P, Roy A, Dal Cin P, Neuberg DS, Monti S, Pinkus GS, Shipp MA, Rodig SJ (2012) Immunohistochemical detection of MYC-driven diffuse large B-cell lymphomas. *PLoS One* 7: e33813

Lan Q, Liu PY, Haase J, Bell JL, Huttelmaier S, Liu T (2019) The critical role of RNA m(6)A methylation in cancer. *Cancer Res* 79: 1285 – 1292

Li A, Chen YS, Ping XL, Yang X, Xiao W, Yang Y, Sun HY, Zhu Q, Baidya P, Wang X *et al* (2017a) Cytoplasmic m(6)A reader YTHDF3 promotes mRNA translation. *Cell Res* 27: 444 – 447

Li Z, Weng H, Su R, Weng X, Zuo Z, Li C, Huang H, Nachtergaele S, Dong L, Hu C *et al* (2017b) FTO plays an oncogenic role in acute myeloid leukemia as a N(6)-methyladenosine RNA demethylase. *Cancer Cell* 31: 127 – 141

Li S, Huang D, Shen S, Cai Y, Xing S, Wu G, Jiang Z, Hao Y, Yuan M, Wang N *et al* (2020) Myc-mediated SDHA acetylation triggers epigenetic regulation of gene expression and tumorigenesis. *Nat Metab* 2: 256 – 269

Lin CY, Loven J, Rahl PB, Paranal RM, Burge CB, Bradner JE, Lee TI, Young RA (2012) Transcriptional amplification in tumor cells with elevated c-Myc. *Cell* 151: 56 – 67

Lin S, Choe J, Du P, Triboulet R, Gregory RI (2016) The m(6)A methyltransferase METTL3 promotes translation in human cancer cells. *Mol Cell* 62: 335 – 345

Luscher B, Vervoorts J (2012) Regulation of gene transcription by the oncoprotein MYC. *Gene* 494: 145 – 160

Melstrom L, Chen J (2020) RNA N(6)-methyladenosine modification in solid tumors: new therapeutic frontiers. *Cancer Gene Ther* 27: 625 – 633

Meyer KD, Jaffrey SR (2017) Rethinking m(6)A readers, writers, and erasers. *Annu Rev Cell Dev Biol* 33: 319 – 342

Nie Z, Hu G, Wei G, Cui K, Yamane A, Resch W, Wang R, Green DR, Tessarollo L, Casellas R *et al* (2012) c-Myc is a universal amplifier of expressed genes in lymphocytes and embryonic stem cells. *Cell* 151: 68 – 79

Nishizawa Y, Konno M, Asai A, Koseki J, Kawamoto K, Miyoshi N, Takahashi H, Nishida N, Haraguchi N, Sakai D *et al* (2018) Oncogene c-Myc promotes epitranscriptome m(6)A reader YTHDF1 expression in colorectal cancer. *Oncotarget* 9: 7476 – 7486

Niu Y, Zhao X, Wu YS, Li MM, Wang XJ, Yang YG (2013) N6-methyl-adenosine (m6A) in RNA: an old modification with a novel epigenetic function. *Genomics Proteomics Bioinformatics* 11: 8 – 17

O'Connell BC, Cheung AF, Simkevich CP, Tam W, Ren X, Mateyak MK, Sedivy JM (2003) A large scale genetic analysis of c-Myc-regulated gene expression patterns. *J Biol Chem* 278: 12563 – 12573

Pajic A, Spitkovsky D, Christoph B, Kempkes B, Schuhmacher M, Staege MS, Brielmeier M, Ellwart J, Kohlhuber F, Bornkamm GW *et al* (2000) Cell cycle activation by c-myc in a burkitt lymphoma model cell line. *Int J Cancer* 87: 787 – 793

Posternak V, Ung MH, Cheng C, Cole MD (2017) MYC mediates mRNA Cap methylation of canonical Wnt/beta-catenin signaling transcripts by recruiting CDK7 and RNA methyltransferase. *Mol Cancer Res* 15: 213 – 224

Sabo A, Kress TR, Pelizzola M, de Pretis S, Gorski MM, Tesi A, Morelli MJ, Bora P, Doni M, Verrecchia A *et al* (2014) Selective transcriptional regulation by Myc in cellular growth control and lymphomagenesis. *Nature* 511: 488 – 492

Savage KJ, Johnson NA, Ben-Neriah S, Connors JM, Sehn LH, Farinha P, Horsman DE, Gascoyne RD (2009) MYC gene rearrangements are associated with a poor prognosis in diffuse large B-cell lymphoma patients treated with R-CHOP chemotherapy. *Blood* 114: 3533 – 3537

Schuhmacher M, Staege MS, Pajic A, Polack A, Weidle UH, Bornkamm GW, Eick D, Kohlhuber F (1999) Control of cell growth by c-Myc in the absence of cell division. *Curr Biol* 9: 1255 – 1258

Shi H, Wang X, Lu Z, Zhao BS, Ma H, Hsu PJ, Liu C, He C (2017) YTHDF3 facilitates translation and decay of N(6)-methyladenosine-modified RNA. *Cell Res* 27: 315 – 328

Shi H, Wei J, He C (2019) Where, when, and how: context-dependent functions of rna methylation writers, readers, and erasers. *Mol Cell* 74: 640 – 650

Singh K, Lin J, Zhong Y, Burcul A, Mohan P, Jiang M, Sun L, Yong-Gonzalez V, Viale A, Cross JR *et al* (2019) c-MYC regulates mRNA translation efficiency and start-site selection in lymphoma. *J Exp Med* 216: 1509 – 1524

Snyder M, Gerstein M, Weissman S, Farnham P, Struhl K (2011) Gene Expression Omnibus GSE31477 (https://www.ncbi.nlm.nih.gov/geo/query/acc.cgi?acc=GSE31477) [DATASET]

Su R, Dong L, Li C, Nachtergaele S, Wunderlich M, Qing Y, Deng X, Wang Y, Weng X, Hu C *et al* (2018) R-2HG exhibits anti-tumor activity by targeting FTO/m(6)A/MYC/CEBPA signaling. *Cell* 172: 90 – 105

Tu WB, Shiah YJ, Lourenco C, Mullen PJ, Dingar D, Redel C, Tamachi A, Ba-Alawi W, Aman A, Al-Awar R *et al* (2018) MYC interacts with the G9a histone methyltransferase to drive transcriptional repression and tumorigenesis. *Cancer Cell* 34: 579 – 595

Walz S, Lorenzin F, Morton J, Wiese KE, von Eyss B, Herold S, Rycak L, Dumay-Odelot H, Karim S, Bartkuhn M *et al* (2014) Activation and repression by oncogenic MYC shape tumour-specific gene expression profiles. *Nature* 511: 483 – 487

Weng H, Huang H, Wu H, Qin X, Zhao BS, Dong L, Shi H, Skibbe J, Shen C, Hu C *et al* (2018) METTL14 inhibits hematopoietic stem/progenitor differentiation and promotes leukemogenesis via mRNA m(6)A modification. *Cell Stem Cell* 22: 191 – 205

Wu G, Yuan M, Shen S, Ma X, Fang J, Zhu L, Sun L, Liu Z, He X, Huang D *et al* (2017) Menin enhances c-Myc-mediated transcription to promote cancer progression. *Nat Commun* 8: 15278

Yang Y, Hsu PJ, Chen YS, Yang YG (2018) Dynamic transcriptomic m(6)A decoration: writers, erasers, readers and functions in RNA metabolism. *Cell Res* 28: 616 – 624

Yang S, Wei J, Cui YH, Park G, Shah P, Deng Y, Aplin AE, Lu Z, Hwang S, He C *et al* (2019) m(6)A mRNA demethylase FTO regulates melanoma tumorigenicity and response to anti-PD-1 blockade. *Nat Commun* 10: 2782

Zeller KI, Zhao X, Lee CW, Chiu KP, Yao F, Yustein JT, Ooi HS, Orlov YL, Shahab A, Yong HC *et al* (2006) Global mapping of c-Myc binding sites and target gene networks in human B cells. *Proc Natl Acad Sci USA* 103: 17834 – 17839

Zhang C, Samanta D, Lu H, Bullen JW, Zhang H, Chen I, He X, Semenza GL (2016a) Hypoxia induces the breast cancer stem cell phenotype by HIF-dependent and ALKBH5-mediated m(6)A-demethylation of NANOG mRNA. *Proc Natl Acad Sci USA* 113: E2047 – E2056

Zhang C, Zhi WI, Lu H, Samanta D, Chen I, Gabrielson E, Semenza GL (2016b) Hypoxia-inducible factors regulate pluripotency factor expression by ZNF217- and ALKBH5-mediated modulation of RNA methylation in breast cancer cells. *Oncotarget* 7: 64527 – 64542

Zhang S, Zhao BS, Zhou A, Lin K, Zheng S, Lu Z, Chen Y, Sulman EP, Xie K, Bogler O *et al* (2017) m(6)A demethylase ALKBH5 maintains tumorigenicity of glioblastoma stem-like cells by sustaining FOXM1 expression and cell proliferation program. *Cancer Cell* 31: 591 – 606